



The influences of the variable speed and internal die geometry on the performance of two commercial soluble oils in the drawing process of pure copper fine wire

Gustavo Aristides Santana Martínez¹ · Oscar Rodriguez-Alabanda² · Umberto Prisco³ · Marius Tintelecan⁴ · Leonardo Kyo Kabayama⁵

Received: 7 June 2021 / Accepted: 30 September 2021 / Published online: 18 October 2021
© The Author(s) 2021

Abstract

The cold wiredrawing process constitutes a classical-tribological system in which a stationary tribe-element (die) is in contact with a tribe-element in relative motion (wire) and both interacting with the interfacial tribe-element (lubricant). This condition is reflected in the effect of friction as a function of the drawing speed and temperature, and directly affects the wearing of the surface into the die and the final quality on the drawn wire. The aim of this work has been to determine the best conditions to process ETP-copper using two different types of oil/water emulsion lubricants. For this purpose, six different die geometries have been proposed and a set of tests have been carried out at different speeds (between 1 and 21 m/s) to determine those combinations that give a lower value in the required drawing force (F_d). The experiments allowed to know the friction coefficient (μ), the temperature profile inside the drawing die and in the lubricant and also the mean roughness (Ra) in the drawn product. The results have shown that drawing speeds above 10 m/s significantly decrease the drawing force and, as a consequence, the friction effect on the interface. The best results have been achieved in the combinations of the lower die angle ($2\beta = 14^\circ$) with drawing speeds between 17 and 18 m/s with both types of lubricants used, obtaining the lower values of the friction coefficient between $\mu = 0.10$ – 0.15 with the lubricant type D (Agip S234-60 oil at 7% concentration). It has been found that those tests carried out with dies with a smaller approach angle have generally made it possible to obtain better qualities in the final product. Additionally, FEM simulations have been done to analyse those cases with the lower values of μ , throwing values of F_d that are consistent with those measured in the experimental setting and allowing to better understand the behavior of the material as it passes through the die.

Keywords Wiredrawing · Die geometry · Tribology · Lubricant · Friction coefficient

✉ Oscar Rodriguez-Alabanda
orodriguez@uco.es

Gustavo Aristides Santana Martínez
gustavo.martinez@usp.br

Umberto Prisco
umberto.prisco@unina.it

Marius Tintelecan
marius.tintelecan@ipm.utcluj.ro

Leonardo Kyo Kabayama
lkabayama@unifei.edu.br

² Area of Manufacturing Processes - Department of Mechanics, University of Córdoba, Carretera Madrid-Cádiz, km 396, 14071 Córdoba, Spain

³ Department of Chemical, Materials and Production Engineering, University of Napoli Federico II, Piazzale Tecchio 80, 80125 Napoli, Italy

⁴ Technical University of Cluj-Napoca, 28 Memorandumului Street, 400114 Cluj-Napoca, Romania

⁵ Institute of Mechanical Engineering, Federal University of Itajubá-UNIFEI, Itajubá 37500-903, Brazil

¹ Engineering School of Lorena, University of São Paulo-USP, Lorena 12602-810, Brazil

1 Introduction

In the production of metal wire by cold wire drawing process the die angle (2β), the cross-sectional area reduction (r), the process speed (v), and the friction coefficient (μ) have a major influence over the required drawing force (F_d), and thus the lubrication regime is a key factor in the process. The process condition, mainly defined by these geometric and technological parameters, directly affects the wear of the drawing die, the mechanical properties of the drawn wire and its final quality depends on them.

In order to improve the wire drawing process, the tribological system must be adequate to minimize the negative effects caused by the inherent wire/die metallic contact, and conditions for low friction must be achieved at the wire/die interface. For this purpose, lubricant coatings based on phosphates or stearates (dry wire drawing) or soluble oil emulsions (wet drawing) are commonly used [1]. The internal die geometry, the wire material, and the drawing speed will determine which should be the characteristics of the most appropriate lubricant to be used for the process.

In the internal drawing die design, the approach angle (2β) characterizes the reduction zone as the most important region in which the total reduction of the wire area occurs. The bearing length zone (H_c) into the die performs the final diameter size of the drawn wire and guarantees the final roundness, straightness and surface smoothness of the product [2]. The condition of the tribological system inside the die largely compromises all these characteristics in the final processed product but also depends directly on the geometric and technological parameters mentioned above.

The Fig. 1 describes a simple graphical representation of the main geometric variables in the wire drawing process and the wire drawing force (F_d) can be calculated as the product of drawing stress and the cross-sectional area of the drawn wire, $F_d = \sigma_d \cdot A$.

Another widely studied aspect, concerning the geometric characterization and its influence on the tribological condition of the process, is delta form factor or relationship (Δ). This parameter characterizes the deformation of metal in the operating cone of the die (Eq. (1)) as a function of the reduction ratio and defines the relationship between the reduction (r) and the die semi-angle (β), consequently affecting the drawing force (F_d) and friction condition in the interface. The area of the cross section of the initial wire is noted as A_i while A_f is the area of the cross section of the drawn wire (Eq. (2)). Also, the total contact length (L) is defined on the Eq. (3).

$$\Delta = \frac{\beta}{r} \left[(1 + \sqrt{1-r})^2 \right] \quad (1)$$

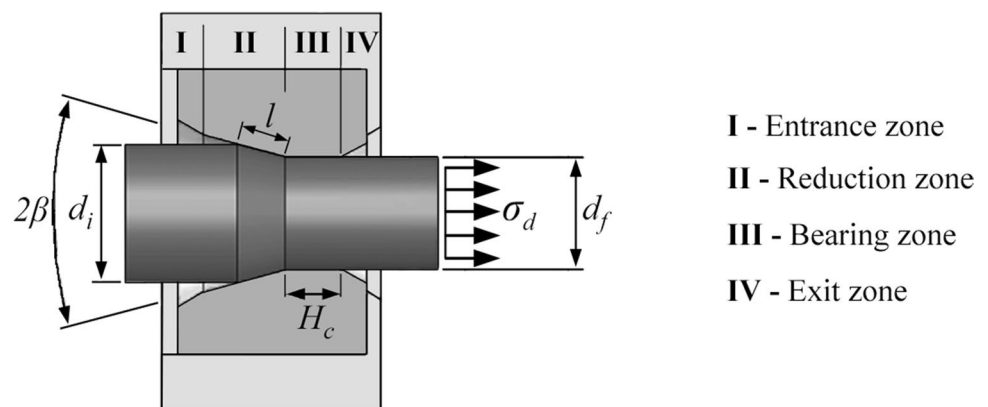
$$r = 1 - \frac{A_f}{A_i} \quad (2)$$

$$L = \left[\frac{r_i - r_f}{\tan \beta} \right] + H_c \quad \text{where } l = \frac{d_i - d_f}{2 \sin \beta} = \frac{r_i - r_f}{\tan \beta} \quad (3)$$

1.1 The role of friction in the wire drawing process

In the wire drawing process, the total work in a single pass can be decomposed in three components: the work required to homogeneously reduce the cross section of the wire (i), the inhomogeneous work consumed in changes of direction of the flow of deformed material the work to overcome (ii), and the friction effect at the interface (iii). These three components constitute the total work that the drawing stress (σ_d) must save for the wire to pass through the die. The inhomogeneous additional work component is closely related with the die geometry, diminishing when the approach angle is lower. For a low area reduction, most of the energy is spent as friction work, and the redundant work is relatively low

Fig. 1 Geometric variables and the main zones in the wire drawing process



when $2 < \Delta < 3$ [3]. Under normal conditions, friction effect constitutes nearly 20% of losses while 12% is due to the additional-redundant work. Typically, a redundant work factor (ϕ) is defined as a function of the die geometry. However, the additional component of the drawing stress caused by redundant work is not only a function of the die geometry but also of the ductility of the drawn metal [4]. Although this component has been yet defined and included in the analytical model based on the slab method [5, 6], it must be noted that it is a complex factor that is determined as a consequence of the flow and internal dislocations that occur in the deformed material and that this model does not allow analysis. This lack can be covered by the finite element method (FEM), which allows modeling and simulating the wiredrawing process, constituting a perfect complement to experimentation since it eases to understand the material flow during the process.

The friction effect in the process increases the temperature in the interface. This heating effect usually leads to the deterioration of the lubrication conditions conducting to cause premature wear of the die, worsening the quality of the drawn product and even causing the wire to break. Thus, the role of the lubricant and the optimization of the tribo-system is a key for a successful process. In this sense, previous works studied the effect of hydrodynamic conditions in wiredrawing. Muskalski’s previous work [7] described and simulated this effect as a phenomenon in which the molecules of lubricant adhere to the wire surface going into the pressure chamber as a thin gap layer between wire and die surfaces. In another recent work, Suliga [8] empirically determined that hydrodynamic lubrication allows to get the optimum tribological conditions at the wire/die interface leading to obtain better results in the multi-stage wiredrawing process of medium carbon zinc-coated steel wires.

In this sense, Avitzur [9] defined the value of the friction coefficient (μ), that essentially constitutes the tribological condition in the process, as a function of the approach semi-angle (β), the wire reduction, the yield limit of the metal to be drawn (σ_{0y}) and the drawing stress (σ_d). Equation (4) shows the dependence of μ on both the geometry of the die and the plastic condition of the metal to be drawn and allows the calculation of this coefficient for certain process and material conditions.

On the other hand, it is important to consider that the central breaks or chevron-shaped inner defects are one of the most common break cause in wiredrawing process and it has been analyzed in the work developed by Bitkov [10]. In this line, both works of Godfrey [11] and Nakagiri [12] numerically and experimentally demonstrated the great influence of the contact length (l) and initial wire diameter (d_i) in the apparition of inner defects causing break of the wire. When the ratio l/d_i is in the range of 0.5–0.7, it prevents central vacuum growth thus avoiding breaks of the wire due to this phenomenon.

1.2 Background

Many previous works consulted demonstrated the great importance of knowing reliably the value of the friction coefficient μ to be able to study analytically or numerically the wiredrawing process. It is so that, by the use of numerical models and methods, Chen and Huang [3] and Majzooobi et al. [4] determined that 2β , Hc and the temperature profile into the die have a significant effect on the drawing process, but it is very important to consider the effect of the wire-die contact length (l) which determines the contact surface at the interface and has a direct effect on the lubrication conditions and, as a consequence, on the value of the friction coefficient μ , involved in the process. Another consulted works demonstrated the feasibility of the use of FEM applied to model the wiredrawing process and focused on the improvement of the geometry of the die [13], on the analysis of the strain distribution in the wire during the process [14] or even to analyze the distribution of residual stresses accumulated in the product once it has been shaped [15], among other output variables. On the other hand, considering all the input factors previously exposed, the effect of drawing speed (v) on the tribological system must be considered since previous works demonstrated that, at high drawing speeds, a localized and intense heating effect is implied in the contact zone which can be detrimental to maintain the properties of the lubricant, worsening the tribological conditions [16, 17].

It should be noted that many of the previous works consulted are mainly focused on the study of the influence of the geometrical parameters involved in the process [18–21] and some of them on the objective directed to the optimization of the multi-stage drawing processes in terms of the

$$\mu = \frac{\sigma_{0y} \cdot \left(\frac{\sigma_{bp}}{\sigma_0} + 2 \cdot f(\beta) \cdot \ln \frac{r_i}{r_f} + \frac{2}{\sqrt{3}} \cdot \left(\frac{\beta}{\sin^2 \beta} - \cot \beta \right) \right) - \sigma_d}{2 \cdot \left(\left(\frac{H_c}{r_f} \cdot \sigma_d \right) - \left\{ \sigma_{0y} \cdot \left[\cot \beta \cdot \left(1 - \frac{\sigma_{bp}}{\sigma_{0y}} - \ln \frac{r_i}{r_f} \right) \cdot \ln \frac{r_i}{r_f} + \frac{H_c}{r_f} \right] \right\} \right)} \quad \text{where } f(\beta) = \frac{\left\{ 1 - \cos \beta \cdot \sqrt{1 - \frac{11}{12} \cdot \sin^2 \beta} + \frac{1}{\sqrt{11 \cdot 12}} \cdot \ln \frac{1 + \sqrt{\frac{11}{12}}}{\sqrt{\frac{11}{12} \cdot \cos \beta + \sqrt{1 - \frac{11}{12} \cdot \sin^2 \beta}}} \right\}}{\sin^2 \beta} \tag{4}$$

die geometry and the number of passes to be carried out in the in-line wiredrawing process [22–24]. Although some of these works describe the use of emulsions based on soluble oils as a common solution in the wiredrawing process of non-ferrous metals and alloys and implement the friction coefficient (μ) for the process analysis, none of them have defined and experimentally studied their own tribological system in order to determine the best conditions for the best optimization of this key parameter. Also, very few works [25] were found on the study and consideration of the interdependence between the used lubricant, the die geometry, and the drawing speed to determine the best tribological condition in the process under study.

Summarizing, the cold wiredrawing process constitutes a classical-tribological system in which is crucial to understand the role of all: (i) the stationary tribe-element (die), (ii) the interfacial tribe-element (lubricant), and (iii) the wire tribe-element in relative motion. Interfacial tribe-element affects the effect of friction, influencing the wearing of tool surface and the quality on the drawn wire surface, even affecting the mechanical properties of the final product.

The present work initially focusses on the empirical study to determine the best tribological conditions in the wiredrawing process of the commercial annealed electrolytic tough pitch 99.94% copper (Cu-ETP). In this first part of the work, the influence of drawing speed and internal die geometry on the performance of two commercial soluble oil emulsions was considered to determine the best condition from the point of view of friction effect in the process. Values of a minimum friction coefficient between $\mu=0.103$ and $\mu=0.145$ have been obtained from the experiments with two different lubricants. To complement the experimental results, the lowest values of μ , obtained with each one of the two different lubricants used, were implemented on a numerical model of the process implemented by FEM. The FEM simulations have allowed understanding the behavior of the material during its deformation, in addition to checking the

coherence of the values of the drawing force observed in the simulations with respect to those measured in the experiments. Finally, the results have shown that the die 1420 has thrown best results with the two lubricants used since the values of friction coefficient, obtained as a function of the measured drawing force (F_d), are generally lower than those obtained with the other different die geometries. Into the bargain, it has been found that the effectiveness of the lubricant LUB C is generally higher, offering better friction conditions than the other lubricant for all the combinations of die geometry and speed studied. Complementarily, a detailed study of the evolution of axial and radial stresses inside the drawing die made by numerical simulation has been added, corresponding to the best friction conditions determined for each of the two lubricants object of study.

2 Materials and methods

2.1 The experimental setting and geometrical data

For the understanding of the water-soluble oil lubricant performance, experimental tests and FEM simulations have been conducted. In the experimental work, a horizontal single die wiredrawing machine (bull block wiredrawing machine) with variable speed from 1 to 23 m/s was instrumented to record the drawing speed (v), drawing force (F_d), and the temperature of the die (T_{die}) and lubricant chamber (T_{lub}). In the experiments, the drawing force (F_d) was measured by a load cell system disposed on the die as is shown in Fig. 2. The nominal capacity of the load cell was equal to 4 kN and its sensitivity to 10 mV/VDC. Also, two TP-K1 thermocouples of 0.5-mm diameter were used to measure the temperature inside the die during the drawing tests. The main thermocouple (sensor 1) was inserted into the dies near the end of the deformation zone and at the beginning of the bearing. Their radial distance from the die axis was equal to 3.75 mm,

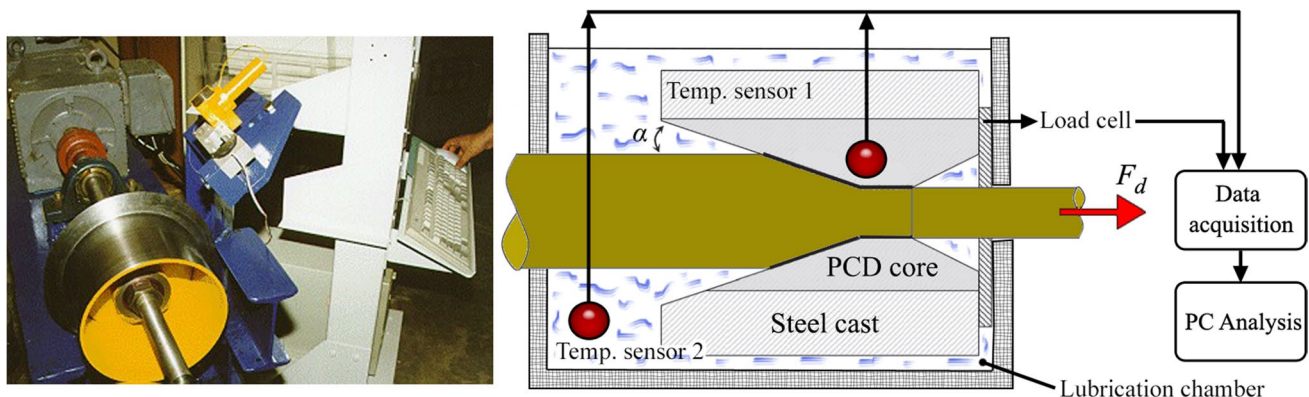


Fig. 2 The wiredrawing machine (own construction) and sensor setup used in the experiments

approximately located at 1.5 mm from the wire-die interface. The second thermocouple (sensor 2) was inserted into the lubrication chamber, near the die. This setting is shown in Fig. 2. All measurements were done in a steady-state condition reached after about 1–2 min from the beginning of each test as the average values taken for 30 s at a sampling rate of 10 Hz.

Two different commercial soluble oil (water-miscible) were studied. The manufacturers of both, LUB C (Agena, Agefil E505/N, Nova Iguacú, Brazil) and LUB D (Agip, S234-60, Abuja, Nigeria), recommend a concentration of 7% of oil concentration in the emulsion for its use in the wiredrawing process.

To estimate the influence of the tool geometry on the performance of each one of the lubricants objects of the present study, six polycrystalline diamond (PCD) dies have been used with internal geometry composed by a reduction zone with an approach angle 2β of 14° and 18° . The bearing region length (H_c) has been established as a 20% (short H_c), 35% (medium H_c), and 50% (long H_c) of the final wire diameter (d_f) in the different dies used in the experiments. The PCD dies have as common dimensions that are summarized in the Table 1: the input diameter (d_i), the conical entrance zone with 60° , the exit zone equal to 40° and the final diameter (d_f). The dimensional accuracy of the internal geometry of the PCD die was checked with a Taylor-Hobson profilographic equipment (Form Talysurf Laser, Taylor-Hobson, Leicester, UK).

The wire/die contact length ratio (l/d_i), internal total contact length (L), delta parameter (Δ), and redundant work factor (ϕ) of PCD dies resulting from geometrical parameters have been determined by the Eqs. (1), (2), (3), (4), (5), and (6). The contact length explains which is the area of contact between wire/die that the lubricant needs maintain separated, and ϕ resumes the die drag capability that maintains lubricant in the interface.

$$\frac{l}{d_i} = \frac{(d_i - d_f)}{2 \cdot d_i \cdot \sin \beta} \tag{5}$$

$$\phi = 0.88 + 0.12 \cdot \frac{\bar{d}}{l} \text{ were } \bar{d} = \frac{d_i - d_f}{2} \tag{6}$$

Table 1 Geometry of the dies used in the experiments

| Die | d_i (mm) | I | 2β ($^\circ$) | H_c (% d_f) | IV | d_f (mm) | l/d_i | L (mm) | Δ | Φ |
|------|------------|------------|-----------------------|------------------|------------|------------|---------|----------|----------|--------|
| 1420 | 0.5 | 60° | 14 | 20 | 40° | 0.45 | 0.41 | 0.29 | 2.32 | 1.62 |
| 1435 | | | 14 | 35 | | | | 0.36 | | |
| 1450 | | | 14 | 50 | | | | 0.43 | | |
| 1820 | | | 18 | 20 | | | 0.31 | 0.25 | 2.98 | 1.8 |
| 1835 | | | 18 | 35 | | | | 0.32 | | |
| 1850 | | | 18 | 50 | | | | 0.38 | | |

2.2 The mechanical properties of the Cu-ETP commercial wire

In the experiments, a 0.5-mm diameter wire of commercial electrolytic tough pitch copper (Cu-ETP of 99.94% purity), not pickled and totally exempts of any superficial oxide, has been processed by drawing up to a diameter of 0.45 mm in one single pass. The mechanical properties of the initial wire have been determined from the tests using an AG-250kN Xplus Shimadzu equipment (Shimadzu Europa GmbH, Duisburg, Germany) mounting an extensometer directly attached to the specimen. The tests have thrown values for the elastic modulus $E = 140,001.92$ MPa, yield strength $\sigma_{y,0.2\%} = 143$ MPa and break limit $\sigma_r = 349.04$ MPa. The stress/strain curves obtained from the tests are shown in Fig. 3 and have been implemented to define the material behavior in the FEM simulations.

2.3 The FEM simulations

Once the experimental study has been carried out and the lowest values of the friction coefficient (μ) have been determined, the best conditions obtained for each type of lubricant have been modeled in the Deform2D software preprocessor [26]. For this FEM models, an axisymmetric condition has been considered. The wire was modeled as an isotropic-deformable and elasto-plastic body while the drawing die was considered as perfectly rigid body. Thus, a finite portion of 25-mm length initial wire has been modeled near the die entrance and aligned with the die axis and it has been meshed in a system of isoparametric elements with four nodes (quadrilateral). The model was completed by defining the mechanical properties of the starting material and its behavior model against cold deformation. The preprocessor allowed to implement the effect of those values of the friction coefficient obtained in the experiments. Finally, the movement condition has been defined by the direction of the displacement of the wire in the nodes of its end and the speed at which they travel (speed of the process implemented in each of the experiments under analysis).

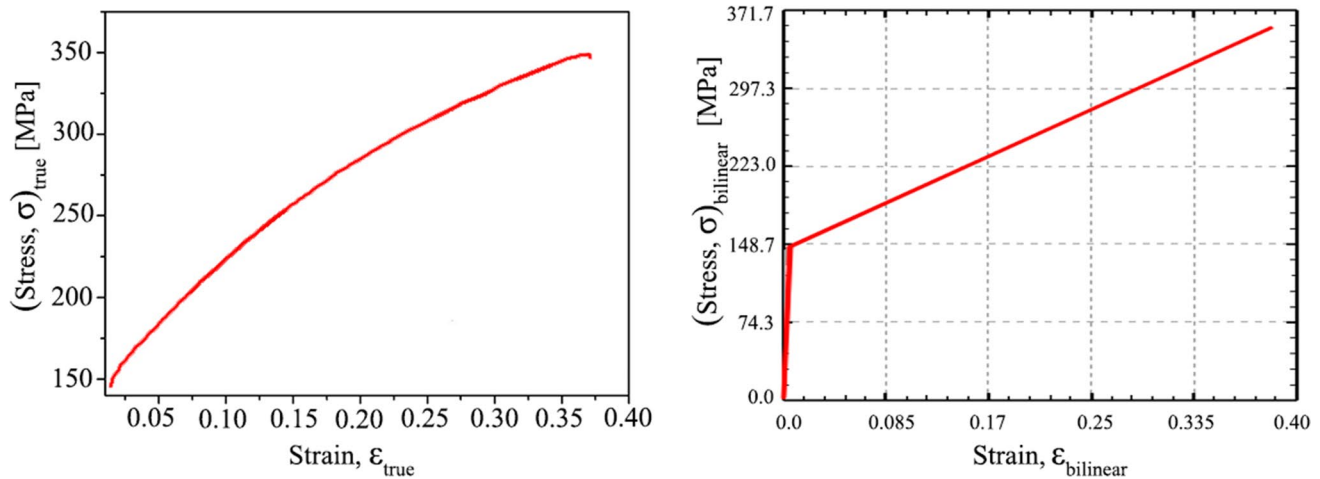


Fig. 3 Experimentally determined stress/strain curve for a specimen of Ø0.5 mm of commercial Cu-ETP copper wire, with 200-mm length at 25 °C. Bilinear model was implemented in FEM simulations

For the better die/lubricant combinations, FEM simulations have been solved in the FEM software processor. Once the numerical solution was obtained, each of both cases has been analyzed in the post-processor to better understand the behavior of the material during its processing. So, the evolution of the radial and axial stresses in the wire as it passes through the different zones of the die has been graphically determined. The drawing force has been graphically simulated, thus being possible to compare this numerical result with the values that have been obtained experimentally in the tests.

3 Results

3.1 Experimental results: temperature profile, friction coefficient and wire surface quality

The experimental work has been focused on the measurements of drawing force (F_d) and temperature (T) variations on the die and into the lubricant chamber. The best results were obtained with the use of the lubricant type LUB C and are shown in Fig. 4, where the temperature on the die (T_{die}), the temperature of the lubricant into the flood chamber (T_{lub}), and the drawing force (F_d) are graphically

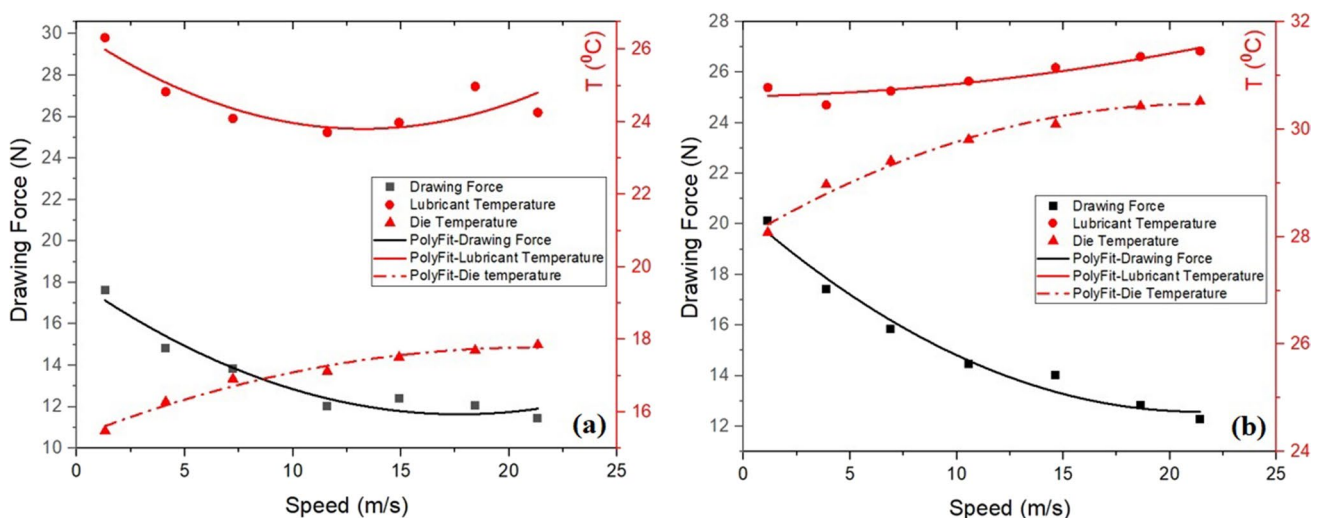


Fig. 4 Temperature profiles and drawing force vs. drawing speed, measured using lubricant type LUB C in the case of dies with $2\beta = 14^\circ$ with different bearing length: (a) $H_c = 20\%$ of d_i and (b) $H_c = 50\%$ of d_i

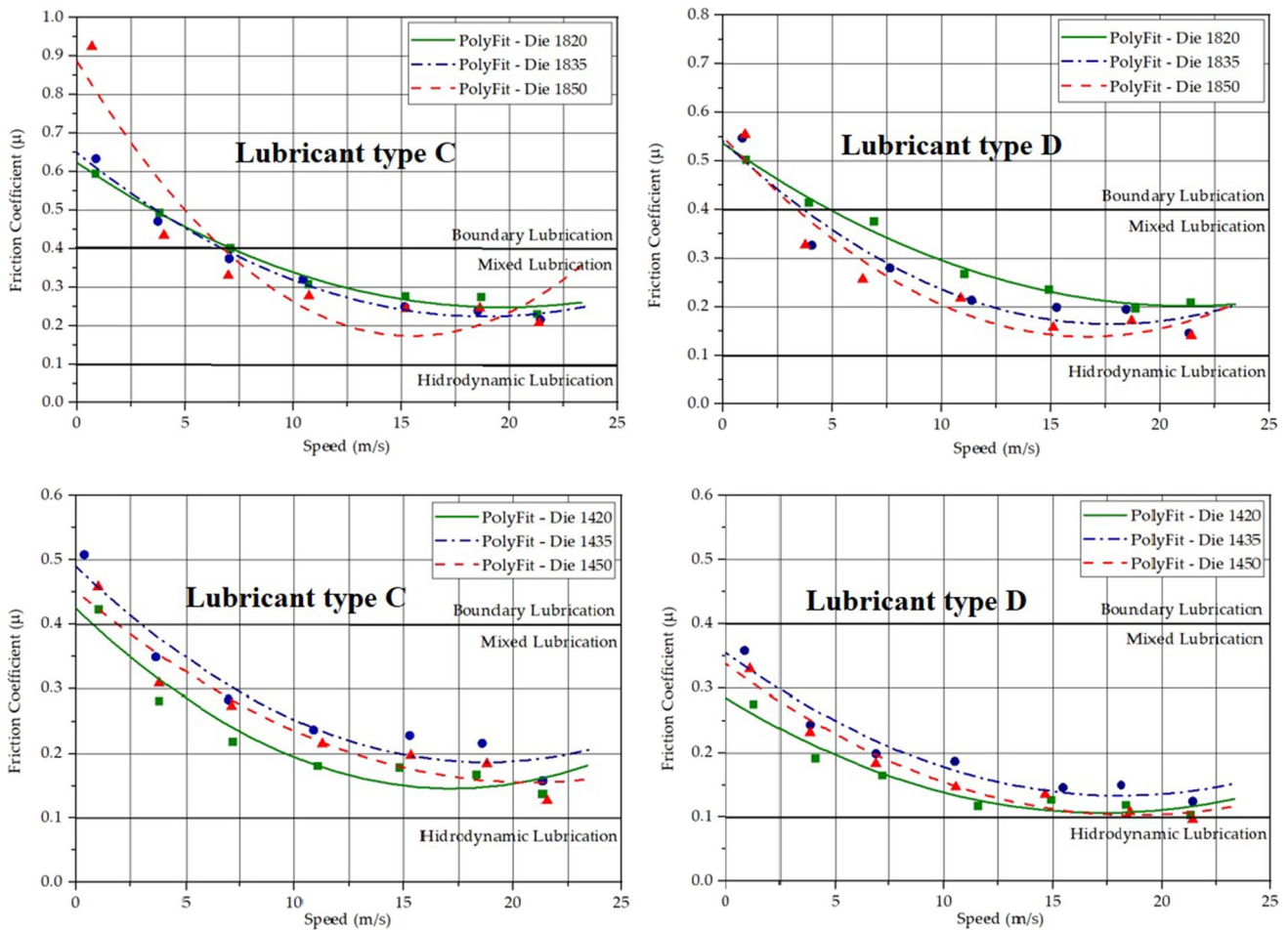


Fig. 5 The experimental variation of the wiredrawing friction coefficient as a function of drawing speed, with six different die geometries and using lubricant types C and D

represented vs. drawing speed (v), since these output parameters have been monitored in both types of different lubricating emulsion mixtures object of study.

It can be seen that, the higher the drawing speed (v), the lower the magnitude of the drawing force (F_d) necessary in the process. An increase in drawing speed of between 10 and 15 m/s implies an ascent of between 2 and 3 °C at the temperature of the drawing die. In both cases, the lubricant temperature remains fairly stable throughout the range of drawing speeds tested.

The full set of six experiments has made it possible to collect drawing force (F_d) measurements and these data have been used to calculate the value of the friction coefficient in each experiment. Figure 5 shows all the results about the experimental variation in the friction coefficient as function of die geometry, lubricant type, and drawing speed. It must to be noted that, as indicated in the consulted bibliography, values of μ among 0.1 to 0.4 define a mixed lubrication condition and values below 0.1 define the hydrodynamic thin film lubrication regime [27, 28].

As the minimum friction coefficient values have been determined by polynomial fitting (Table 2), the corresponding fitting curves show the evolution of the friction coefficient value as a function of the die geometry, drawing speed and lubricant capability to maintain wire/die separated.

The results have shown that both the drawing force (F_d) and the friction coefficient values obtained are lower

Table 2 Results of the minimum value for the friction coefficient obtained from the experiments

| Die | LUB C | | LUB D | |
|------|-----------|-------|-----------|-------|
| | v (m/s) | μ | v (m/s) | μ |
| 1420 | 16.96 | 0.145 | 17.01 | 0.106 |
| 1435 | 18.14 | 0.187 | 18.28 | 0.133 |
| 1450 | 21.00 | 0.155 | 18.32 | 0.103 |
| 1820 | 19.46 | 0.247 | 20.87 | 0.201 |
| 1835 | 18.30 | 0.224 | 18.21 | 0.164 |
| 1850 | 15.60 | 0.172 | 17.03 | 0.138 |

with the lubricant type D than those obtained with type C. This difference has been more accentuated with dies of $2\beta = 14^\circ$, showing drawing force (F_d) values below 14 N at drawing speeds starting from 7.5 m/s. In other words, with practically the same amount of lubricant carted (pulled into the die by the wire) into the interface, the lubricant type D has been more effective in the separation of the wire/die surfaces. It has been possible to see that the die 1420 is the best with both types of lubricant emulsions. It can be deduced that the frictional heat is transmitted through the die going to the lubricant in a great proportion. The capacity to evacuate this heat depends on the type of lubricant emulsion (93% in volume of water) and the geometry of the drawing die. The results have shown that the emulsion reduces the power required in the process by reducing surface friction, dissipating the heat generated while the die accumulates it in a lower proportion. Furthermore, in this first experimental phase in which tests were carried out with 6 different geometries, at 6 different drawing speeds from 1 to 21 m/s and using both lubricants under study, results have been obtained that are near to reach the boundary and mixed regime of lubrication in the wire/die interface.

Additionally, the surface quality of the wires processed by drawing has been verified. In Table 3 are shown the results of the minimum surface roughness measured on the drawn wires.

In terms of the effect of lubricity, the results obtained from the measurements about the mean roughness (Ra) on the surface of the drawn wire have shown better quality level in the experiments performed with the lubricant type LUB D. It is important to note that the surface roughness conditions in the initial wire and the correct performance of the lubricant used in the process could have a significant influence on the quality of end-products produced by drawing (Ra). The experiment has shown that, with the use of lubricant type LUB C, the higher values of Ra have been obtained when the die angle 2β is equal to 14° , while with $2\beta = 18^\circ$ and lubricant type LUB

D allowed to get a better improvement in terms of Ra. If the results obtained are analyzed, it can be concluded that the surface roughness Ra is directly related with the lubricating capacity of the lubricant used: the lower the coefficient of friction at the interface, the better the surface quality obtained in the drawn wire, as can be seen by comparing the data reflected in Tables 2 and 3. The results have shown that, as a general rule, an increase in speed damages the surface of the wire. The lower roughness values were obtained when the bearing length (H_c) was greater and $2\beta = 14^\circ$, except for die 1420 combined with the lubricant LUB C, while for $2\beta = 18^\circ$ the opposite effect seems to occur.

3.2 Results obtained by FEM simulations

Analyzing the evolution of the stresses that are generated in the deformation zone during the wiredrawing process, Yoshida confirmed in his work that the distribution of axial and radial stresses in the deformation zone into the die affects the final dimension and straightness in the wire processed by drawing [29]. There are various factors that influence the axial and radial (die pressure) stresses, and the geometric profile of the die and tribological conditions are the most decisive. To better understand this fact, FEM simulations have been analyzed to understand how the distribution of the radial and axial stresses on the surface and at the center is different as a function of the use of each of the lubricants object of this study.

Figures 6 and 7 enable a better understanding of the behavior of lubricants in the two best conditions determined from the experiments.

Figure 6 shows that the surface (a) and center (b) axial stress are lower with the use of lubricant emulsion LUB D. Its lubricant capacity is explained by the best results in terms of lower values of axial stresses, although the contact length L is 48.27% larger in the die used.

In terms of radial stress distribution into the deformation zone (Fig. 7), the lubricant emulsion LUB D demonstrated the best results. The influence of the contact length L explains the marked increase of the radial stresses caused by the calibration effect into the cylindrical zone H_c . The maximum value of the radial stress is given at the final of region (II), and it reaches a value around 275 MPa (compression) in both surface and center of the die. The behavior of the two better combinations of die/lubricant type compared is quite similar in terms of generated radial stresses, as can be seen in the graphs of Fig. 7.

Table 4 shows the output results that concerned the maximum values of the axial and radial stresses obtained from the FEM simulations and performed for the better combinations die/lubricant (die 1420/LUB C and die 1450/LUB D).

Table 3 Results of the minimum value for the surface roughness measured on the drawn wires

| Die | LUB C | | LUB D | |
|------|------------------------|-------------------------|------------------------|-------------------------|
| | Ra (μm) | | Ra (μm) | |
| | $\varnothing 0.5$ (mm) | $\varnothing 0.45$ (mm) | $\varnothing 0.5$ (mm) | $\varnothing 0.45$ (mm) |
| 1420 | 1.03 | 0.47 | 0.55 | 1.80 |
| 1435 | 1.48 | 0.86 | 0.29 | 0.25 |
| 1450 | 1.19 | 0.95 | 1.36 | 0.26 |
| 1820 | 0.31 | 0.42 | 2.04 | 0.66 |
| 1835 | 0.50 | 0.55 | 0.60 | 0.96 |
| 1850 | 0.98 | 0.97 | 0.55 | 1.90 |

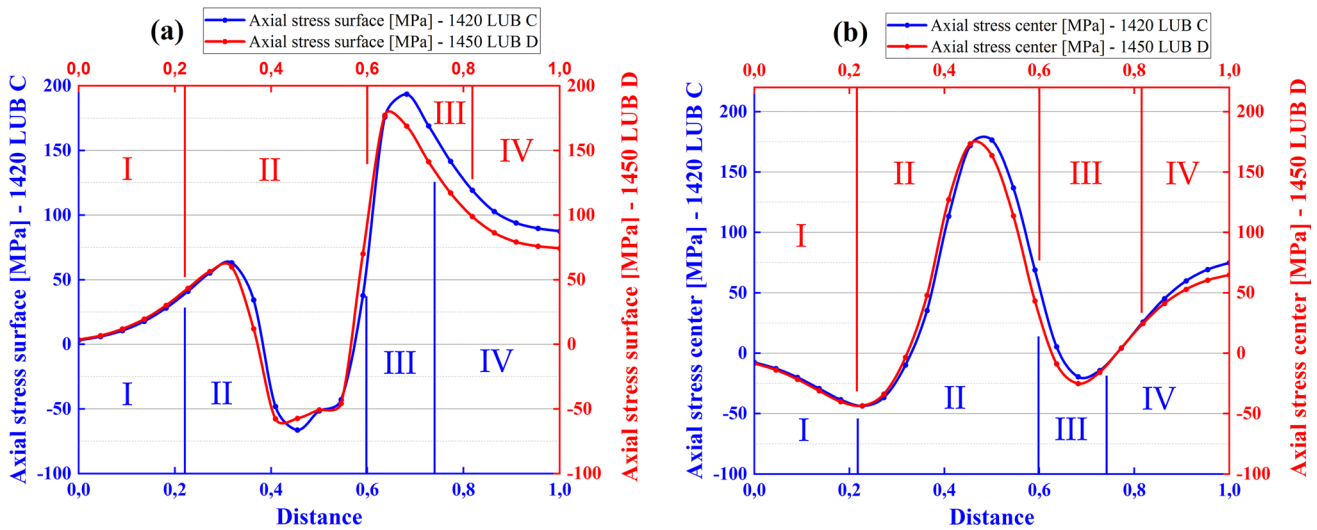


Fig. 6 Axial stress vs distance. Nodes in the surface (a) and center (b) of wire. Comparison between dies 1420 ($2\beta=14^\circ$; $H_c=20\% d_j$; $\mu=0.145$ —LUB C) and 1450 ($2\beta=14^\circ$; $H_c=50\% d_j$; $\mu=0.103$ —LUB D)

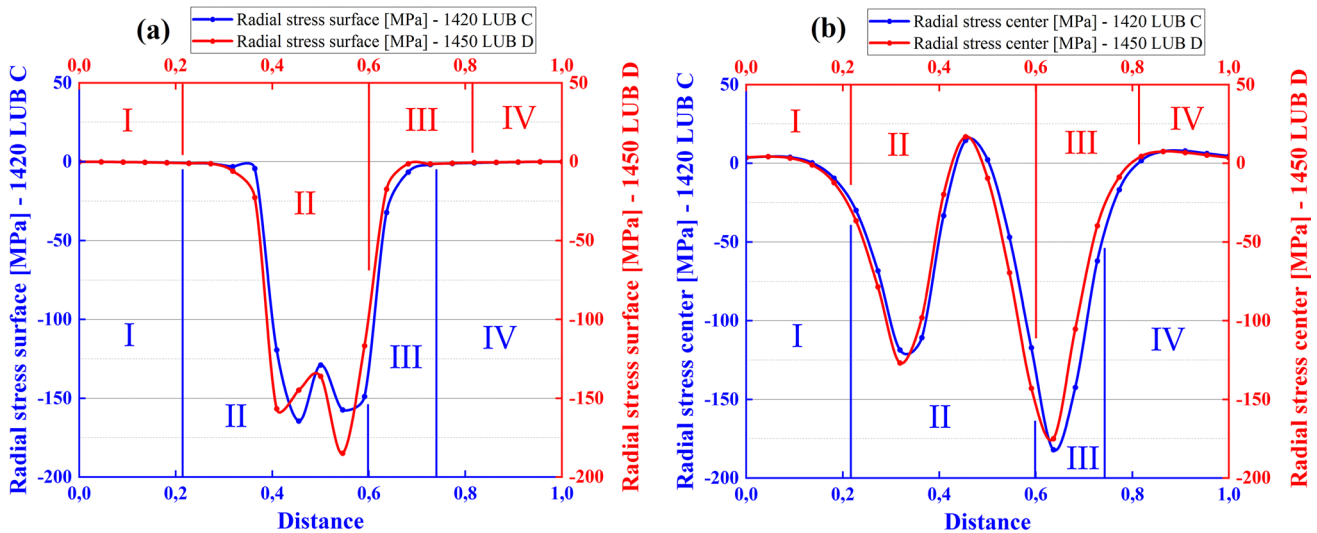


Fig. 7 Radial stress vs distance. Nodes in the surface (a) and center (b) of wire. Comparison between dies 1420 ($2\beta=14^\circ$; $H_c=20\% d_j$; $\mu=0.145$ —LUB C) and 1450 ($2\beta=14^\circ$; $H_c=50\% d_j$; $\mu=0.103$ —LUB D)

Table 4 Maximum values of the axial and radial stresses from the FEM simulations

| Die/Lubricant | μ | $\sigma_{\text{axial max.surface}}$ [MPa] | $\sigma_{\text{axial max.center}}$ [MPa] | $\sigma_{\text{radial max.surface}}$ [MPa] | $\sigma_{\text{radial max.center}}$ [MPa] |
|---------------|-------|---|--|--|---|
| 1420/LUB C | 0.146 | 192.3 | 177.4 | -167.2 | -181.5 |
| 1450/LUB D | 0.103 | 178.5 | 174.8 | -185.3 | -175.2 |

Besides, reading the outputs of the drawing force (F_d) in the FEM simulations, it has been possible to compare them with those values empirically measured to validate the study.

The numerical results of the drawing force (F_d) have been read directly from the tracking graphics as a process output in the Deform2D FEM software, as is shown in Fig. 8.

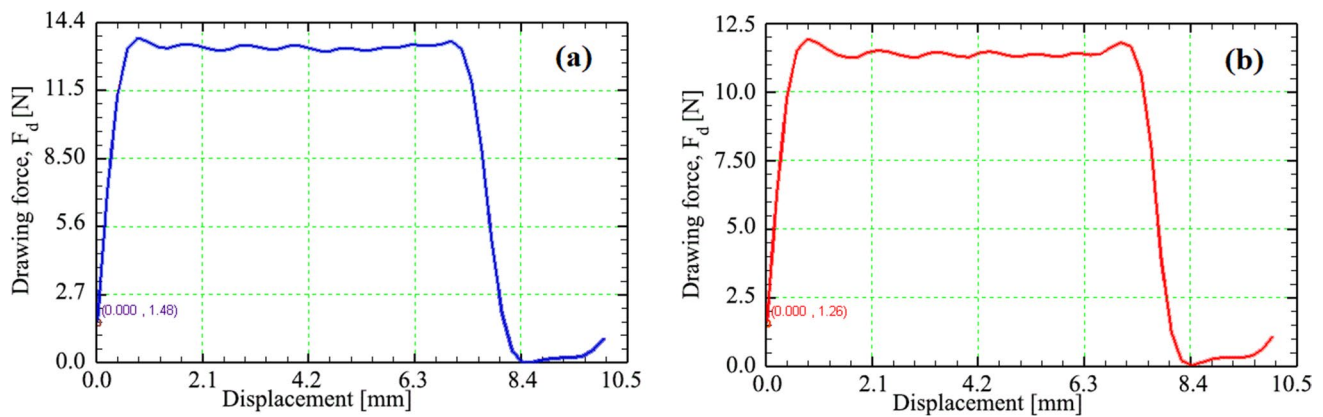


Fig. 8 Drawing force (F_d) as a function of the stroke displacement for a 6-mm length wire: **a** die 1420 ($2\beta=14^\circ$; $H_c=20\% d_i$; $\mu=0.145$ —LUB C) and **b** die 1450 ($2\beta=14^\circ$; $H_c=50\% d_i$; $\mu=0.103$ —LUB D)

Table 5 shows the output results that concerned the values of the drawing force (F_d) that have been obtained from the FEM simulations (Deform2D) compared with those obtained from the experiments (load cell).

Although the solution obtained from the FEM numerical model considers most of the effects produced by the main factors involved in the wire drawing process, the results observed in the simulations for the drawing force (F_d) and drawing stress (σ_d) are very close to the experimental values but slightly lower than those obtained in the experiments, just as expected. Nevertheless, the FEM results of F_d have shown good agreement with those values measured experimentally.

4 Conclusions

In the present work, the wire drawing process of fine copper wire has been experimentally approached with the aim of determining the conditions to achieve a maximum reduction of the effect of friction considering the die angle (2β), calibration length (H_c), drawing speed (v), and two different lubricants generally applicable in copper processing. The main questions concluded from the results of this study are summarized below:

- The lubricant type C, in combination with a die with $2\beta=14^\circ$ and $H_c=0.20 \cdot d_i$, favors the evacuation of the

heat generated through the lubricant/coolant emulsion (T_{lub} between 26 and 30 °C), allowing a lower temperature in the die (T_{die} between 10 and 16 °C).

- The Avitzur equations allowed to calculate the values of the friction coefficient (μ) from the experimental measurements of the drawing force (F_d).
- The polynomial fitting models of the experimental results of μ vs. drawing speed (v) allowed to determine the better conditions to achieve the optimum lubrication regime of the process (the lowest value of μ between die and wire).
- The use of lubricant type LUB C, in combination with $2\beta=14^\circ$ and $H_c=0.20 \cdot d_i$ and working at $v=16.96$ m/s, resulted in a minimum value of the coefficient of friction $\mu=0.145$.
- The use of lubricant type LUB B, in combination with $2\beta=14^\circ$ and $H_c=0.50 \cdot d_i$ and working at $v=18.32$ m/s, resulted in a minimum value of the coefficient of friction $\mu=0.103$ which is the lowest obtained in the experiments.
- In general terms, the lower value of friction coefficient (μ) has been achieved with the lubricant type LUB D, throwing values in the order of $\mu=0.10$ to $\mu=0.13$ with dies with an angle of $2\beta=14^\circ$.
- The lower Ra ($Ra < 0.3 \mu\text{m}$) in the drawn wire have been obtained with the use of dies with $2\beta=14^\circ$ and with the greater calibration lengths ($H_c=35 \div 50\%$ of the d_i), using the lubricant type LUB D.
- For the best combinations ($2\beta=14^\circ$; $H_c=20\% d_i$; $\mu=0.145$ with LUB C and $2\beta=14^\circ$; $H_c=50\% d_i$; $\mu=0.103$ with LUB D), FEM simulations have been implemented to better understand the process conditions and the role of all the stresses and forces involved when this process is in its stationary state.
- The axial and radial stresses profiles have shown a slight dependence on the type of lubricant used, but their values and distribution are mainly affected by the geometry of the die, although it has been observed that the influence of the calibration length on this stress profile is very small.

Table 5 Experimental and numerical values of drawing stress (σ_d) and drawing force (F_d)

| Die/Lubricant | μ | Experimental | | FEM | |
|---------------|-------|--------------|------------------|-----------|------------------|
| | | F_d [N] | σ_d [MPa] | F_d [N] | σ_d [MPa] |
| 1420/LUB C | 0.145 | 13.27 | 83.46 | 12.92 | 81.26 |
| 1450/LUB D | 0.103 | 12.74 | 80.12 | 11.74 | 73.83 |

- The values of the drawing force (F_d) and the consequent drawing stress (σ_d) obtained from the numerical simulations agree with those measured in the experiments, validating the FEM simulations.

Author contribution Conceptualization: G. A. S. M., U. P. and L. K. K.; methodology: G. A. S. M. and O. R-A.; investigation: G. A. S. M., O. R-A. and L. K. K.; resources: G. A. S. M. and O. R-A.; writing (original draft preparation): G. A. S. M. and O. R-A.; final writing—editing and review: O. R-A., U. P., M. T., L. K. K. and G. A. S. M.; supervision: G. A. S. M.

Funding Open Access funding provided thanks to the CRUE-CSIC agreement with Springer Nature.

Data Availability Not applicable.

Code availability Not applicable.

Declarations

Ethics approval and consent to participate Not applicable.

Consent for publication All the authors consent the publication of this work in JAMT.

Competing interests The authors declare no competing interests.

Open Access This article is licensed under a Creative Commons Attribution 4.0 International License, which permits use, sharing, adaptation, distribution and reproduction in any medium or format, as long as you give appropriate credit to the original author(s) and the source, provide a link to the Creative Commons licence, and indicate if changes were made. The images or other third party material in this article are included in the article's Creative Commons licence, unless indicated otherwise in a credit line to the material. If material is not included in the article's Creative Commons licence and your intended use is not permitted by statutory regulation or exceeds the permitted use, you will need to obtain permission directly from the copyright holder. To view a copy of this licence, visit <http://creativecommons.org/licenses/by/4.0/>.

References

- Shemenski RM, Swindells JE, Monaco R (2008) Ferrous wire handbook. The Wire Association International Inc., Guilford, Connecticut
- Siva Naga Teja Ch, Guru Murty N, Satish Reddy P (2016) Finite element analysis of wire drawing process with different die contours. *Int J Sci Eng Adv Technol* 4:134–143
- Antunes S, Sousa OD, Kenji L et al (2018) The wire drawing mechanics of near-equiatomic NiTi SMA 2. Experimental procedure. *Mater Res* 21:1–5. <https://doi.org/10.1590/1980-5373-MR-2017-0944>
- Zhang G-L, Wang Z-W, Zhang S-H et al (2013) A fast optimization approach for multipass wire drawing processes based on the analytical model. *Proc Inst Mech Eng Part B J Eng Manuf* 227:1023–1031. <https://doi.org/10.1177/0954405413481780>
- González Rojas HA, Calvet JV, Bubnovich VI (2008) A new analytical solution for prediction of forward tension in the drawing process. *J Mater Process Technol* 198:93–98. <https://doi.org/10.1016/j.jmatprotec.2007.06.053>
- Rodríguez-Alabanda O, Romero PE, Guerrero-Vaca G, Sevilla L (2018) Software implementation of a new analytical methodology applied to the multi-stage wire drawing process: the case study of the copper wire manufacturing line optimization. *Int J Adv Manuf Technol* 96:2077–2089. <https://doi.org/10.1007/s00170-018-1657-y>
- Muskalski Z, Wiewiórska S (2011) The theoretical analysis of wire drawing process for hydrodynamic friction conditions. *Metall Min Ind* 3:74–78
- Dies H, Suliga M, Wartacz R, Hawryluk M (2020) The multi-stage drawing process of zinc-coated medium-carbon steel wires in conventional and. *Materials (Basel)* 13:1–14. <https://doi.org/10.3390/ma13214871>
- Avitzur B (1983) Handbook of Metal Forming. John Wiley & Sons Inc., New York, NY, USA
- Bitkov VV (2010) Minimization of breaks during drawing thin wire of nonferrous metals. *Russ J Non-Ferrous Met* 51:134–139. <https://doi.org/10.3103/S1067821210020112>
- Godfrey HJ, Richards JF, Sason AS (2000) The benefits of using wiredrawing dies with smaller included angles and long nibs. *Wire J Int* 33:102–113
- Nakagiri A, Yamano T, Konaka M, Asakawa M (2001) Behavior of residual stress and drawing stress in conical-type die and circle-type die drawing by FEM simulation and experiment. *Wire J Int* 34:72–80
- Hassan A, Hashim A (2015) Three dimensional finite element analysis of wire drawing process. *Univers J Mech Eng* 3:71–82. <https://doi.org/10.13189/ujme.2015.030302>
- Lee S, Lee I, Lee S, Lee S (2019) Prediction of effective strain distribution in two-pass drawn wire. *Materials (Basel)* 12:1–13. <https://doi.org/10.3390/ma12233923>
- Dmitriy D (2019) Analysis of residual stress in circular cross-section wires after drawing process. *Procedia Manuf* 37:335–340. <https://doi.org/10.1016/j.promfg.2019.12.056>
- Suliga M, Muskalski Z, Wiewiórska S (2008) The influence of drawing speed on properties of TRIP steel wires. 26:151–154
- Suliga M (2011) The influence of the high drawing speed on mechanical-technological properties of high carbon steel wires. *Arch Metall Mater* 56:823–828. <https://doi.org/10.2478/v10172-011-0091-z>
- Vega G, Haddi A, Imad A (2009) Investigation of process parameters effect on the copper-wire drawing. *Mater Des* 30:3308–3312. <https://doi.org/10.1016/j.matdes.2008.12.006>
- Banda F, Siaminwe L, Mwenda HM (2014) Aspects of die geometry influencing drawability of metals during wire drawing : a literature review. *J Manuf Sci Prod* 14:141–149. <https://doi.org/10.1515/jmsp-2013-0023>
- Sas-Boca IM, Tintelecan M, Pop M et al (2017) The wire drawing process simulation and the optimization of geometry dies. *Procedia Eng* 181:187–192. <https://doi.org/10.1016/j.proeng.2017.02.368>
- Kabayama LK, Taguchi SP, De SU et al (2009) The influence of die geometry on stress distribution by experimental and FEM simulation on electrolytic copper wiredrawing. *Mater Res* 12:281–285
- Lee SK, Lee SB, Kim BM (2010) Process design of multi-stage wet wire drawing for improving the drawing speed for 0.72 wt% C steel wire. *J Mater Process Technol* 210:776–783. <https://doi.org/10.1016/j.jmatprotec.2010.01.007>
- Rodríguez-Alabanda O, Romero PE, Molero E, Guerrero-vaca G (2019) Analysis, validation and optimization of the multi-stage sequential wiredrawing process of EN AW-1370 aluminium. *Metals (Basel)* 9:1–17. <https://doi.org/10.3390/met9091021>
- Lee S, Lee I, Lee S et al (2019) Fabrication of 50.0 μm ultra-fine pure rhodium wire, using a multi-pass wire drawing process, for

- probe card pins. *Materials* (Basel) 12:1–12. <https://doi.org/10.3390/ma12132194>
25. Lima Filho A de P, Ferreira IR, Cataneo FB, et al (2012) Friction and stress evaluation of copper wire drawing under different lubrication conditions. In: 68th ABM Annual Congress. Belo Horizonte, Brazil, pp 3402–3413. ISSN 1516–392X
 26. Fluhner J (2004) Deform2D version 8.1 User's Manual. Scientific Forming Technologies Corporation, Ohio (EE.UU.)
 27. Wilson WRD (1978) Friction and lubrication in bulk metal-forming processes. *J Appl Metalwork* 1:7–19. <https://doi.org/10.1007/BF02833955>
 28. Cheng HS (1992) *Lubrication Regimes*, ASM Handbook Vol.18, Friction, Lubrication, and Wear Technology. ASM International, West Conshohocken, PA, USA
 29. Yoshida K, Ido R, Tamashita T (2002) Effects of back tension and drawing direction on wire properties in copper wire drawing. *Wire J Int* 35:110–115

Publisher's Note Springer Nature remains neutral with regard to jurisdictional claims in published maps and institutional affiliations.